# Chlamydia muridarum Infection Impacts Murine Models of Intestinal Inflammation and Cancer

Glory Leung, DVM,<sup>1,\*,†</sup> Sebastian E Carrasco, DVM, MPVM, MSc, PhD, DACVP,<sup>1,2</sup> Anthony J Mourino, BS,<sup>3</sup> Mert Aydin, MSc,<sup>3</sup> Renata Mammone, VMD, MS, DACVP,<sup>2</sup> Gregory F Sonnenberg, PhD,<sup>4</sup> Gretchen Diehl, PhD,<sup>5</sup> David Artis, PhD,<sup>4,6,7,8</sup> Hiroshi Yano, PhD,<sup>4,6,7,8</sup> Rodolfo J Ricart Arbona, MLAS, DVM, DACLAM,<sup>1,2,\*,‡</sup> and Neil S Lipman, VMD, DACLAM<sup>1,2,‡</sup>

Chlamydia muridarum has reemerged as a prevalent infectious agent in research mouse colonies. Despite its prevalence and ability to persistently colonize the murine gastrointestinal tract, few studies have evaluated the potential impact of C. muridarum on experimental models of gastrointestinal disease. Studies were conducted to evaluate the impact of C. muridarum on the Citrobacter rodentium, Trichuris muris, and Il10-1- mouse models of intestinal inflammation, as well as on tumorigenesis in the ApcMin/+ mouse following administration of dextran sodium sulfate (DSS). Naïve C57BL/6J (B6), B6.129P2-II10<sup>tim1Cgnt</sup>/J (II10<sup>-l-</sup>), and C57BL/6J-ApcMin/J (ApcMin/+) mice were infected with C. muridarum by cohousing with chronic C. muridarum-shedding BALB/cJ mice for 2 weeks; controls were cohoused with C. muridarum-free mice. After cohousing, B6 mice (n = 8 C. muridarum infected and free) were infected with C. rodentium (10 $^{9}$  CFU orally) or T. muris (200 ova orally). Il 10 $^{-1}$  mice (n = 8/group with and without Helicobacter hepaticus [108 CFU/mouse] and with and without C. muridarum) and  $Apc^{Min/+}$  mice (n = 8/group) that received 2% DSS for 7 days in drinking water after cohousing. Mice were euthanized 14 days post-C. rodentium infection, 18 days post-T. muris infection, 60 days post-H. hepaticus infection, or control with Il10-1- mice, and 28 days post-DSS administration to ApcMin/+ mice. The severity of the cecal and colonic lesions was evaluated and graded using a tiered, semiquantitative scoring system. C. muridarum infection attenuated colitis associated with C. rodentium (P = 0.03), had no effect on T. muris-associated pathology (P = 0.22), worsened colitis in  $Il10^{-/-}$  mice in the absence of H. hepaticus (P = 0.007), and reduced chemically induced colonic tumorigenesis in Apc $^{Min/+}$  mice (P = 0.004). Thus, C. muridarum colonization differentially impacts several models of intestinal inflammation and tumorigenesis, and the presence of this bacterium in mouse colonies should be considered as a variable in these experimental readouts.

**Abbreviations and Acronyms:** Apc, adenomatous polyposis coli; B6, C57BL/6J; BCS, body condition score; C, BALB/cJ; DSS, dextran sodium sulfate; IHC, immunohistochemistry; ISH, in situ hybridization; GIT, gastrointestinal tract; MOMP, *Chlamydia* major outer membrane permeabilization

**DOI:** 10.30802/AALAS-JAALAS-25-078

## Introduction

Chlamydia muridarum, a Gram-negative obligate intracellular bacterium, was initially described in the 1940s as mouse pneumonitis virus in mice used to investigate the causes of human respiratory infections. Approximately a decade later, the organism was identified as Chlamydia trachomatis and in the 1990s was reclassified as C. muridarum, the only Chlamydia species known to naturally infect the family Muridae. C. muridarum had not been detected in research mice since these original descriptions,

although it has been used extensively to model genital tract infections in humans caused by *C. trachomatis*.<sup>2</sup>

We recently reported on the unexpected reemergence of *C. muridarum* in research mouse colonies. About a third of the mice imported to our institution, principally from other US and European academic institutions, were infected with *C. muridarum*. Surveys of approximately 900 and 11,000 murine diagnostic and environmental samples submitted to research animal diagnostic laboratories from 120 institutions demonstrated that 16% and 14%, respectively, were quantitative PCR (qPCR) positive for *C. muridarum*. This prevalence is markedly higher than most excluded murine adventitious agents including mouse hepatitis virus and mouse parvovirus, which were recently reported to have less than a 0.3% prevalence.<sup>3</sup>

*C. muridarum* has a 2-stage life cycle consisting of the infectious, nonreplicating elementary body and a replicating, noninfectious reticulate body.<sup>2</sup> Natural transmission is primarily fecal-oral.<sup>4</sup> Natural infection of immunocompetent mouse strains is not associated with clinical signs, while immunocompromised strains develop respiratory signs, weight loss, and pulmonary pathology following natural infection.<sup>4-6</sup> In immunocompetent mice, *C. muridarum* elicits IgG secretion and transient lymphocyte proliferation in draining mesenteric lymph nodes as well as induction of monocytes and activation

Submitted: 13 May 2025. Revision requested: 12 Jun 2025. Accepted: 16 Jul 2025. 

<sup>1</sup>Tri-Institutional Training Program in Laboratory Animal Medicine and Science, Memorial Sloan Kettering Cancer Center, Weill Cornell Medicine, and The Rockefeller University, New York, New York; 

<sup>2</sup>Center of Comparative Medicine and Pathology, Memorial Sloan Kettering Cancer Center and Weill Cornell Medicine, New York, New York; 

<sup>3</sup>The Jackson Laboratory, Bar Harbor, Maine; 

<sup>4</sup>Joan and Sanford I. Weill Department of Medicine, Division of Gastroenterology and Hepatology, Weill Cornell Medicine, Cornell University, New York, New York; 

<sup>5</sup>Memorial Sloan Kettering Cancer Center, New York, New York; 

<sup>6</sup>Jill Roberts Institute for Research in Inflammatory Bowel Disease, Weill Cornell Medicine, Cornell University, New York, New York, 

<sup>7</sup>Friedman Center for Nutrition and Inflammation, Weill Cornell Medicine, Cornell University, New York, NY; and 

<sup>8</sup>Allen Discovery Center for Neuroimmune Interactions, New York, NY

\*Corresponding author. Email: gleung3@uottawa.ca or ricartr@mskcc.org or ipmann@mskcc.org

ˈ †Current affiliation: Animal Care and Veterinary Service, University of Ottawa, Ottawa. Ontario

‡These authors contributed equally to this study

of T-cell subsets resulting in a significant reduction of *C. mu-ridarum* within the gut, but the bacterium persists in the cecum and large intestine while being shed chronically in the feces.<sup>4,6</sup>

Despite the high prevalence, little is known about the potential confounding effects that C. muridarum infection may have on research models. Since most mouse strains are persistently infected with C. muridarum, which has been shown to elicit both innate and adaptive immune responses, we speculated that *C*. muridarum may impact murine research models used to study intestinal inflammation and neoplasia. Wang et al<sup>7</sup> recently showed that oral inoculation of C. muridarum protects against dextran sodium sulfate (DSS)-induced colitis, likely by promoting IL-22 secretion, a cytokine with strong antimicrobial properties. The DSS-induced model of colitis is only one of many commonly used murine models of intestinal inflammation that could potentially be impacted by C. muridarum. Based on the pathways involved in the pathophysiology of the associated disease, we investigated the impact of *C. muridarum* on the *Citrobacter rodentium*, *Trichuris* muris, and IL-10 knockout models of intestinal inflammation as well as in the Apc<sup>Min/+</sup>mouse model of tumorigenesis.

# **Materials and Methods**

**Experimental models.** To investigate the impact of *C. muridarum* infection on various murine gastrointestinal models, we first infected C57BL/6J, B6.129P2-II10<sup>tm1Cgn</sup>/J (II10<sup>-/-</sup>), and C57BL/6J-Apc<sup>Min</sup>/J (Apc<sup>Min/+</sup>) mice with *C. muridarum* by cohousing with chronically shedding *C. muridarum*-infected BALB/cJ (C) mice for 2 weeks (1 infected C mouse/1-4 naïve experimental mice). Naïve *C. muridarum*-free C mice were cohoused with the same strains as controls. The experimental design and timeline are depicted graphically in Figure 1.

C. muridarum-positive and -negative B6 mice, confirmed by qPCR, were inoculated with either C. rodentium (n = 8/C. muridarum+ or C. muridarum-; 109/CFUs) or T. muris (n = 8/C. muridarum+ or C. muridarum-; 200 ova) via orogastric gavage 14 days after cohousing with C. muridarum-shedding or C. muridarum-free C mice. Fourteen or 18 days post-C. rodentium or post-T. muris infection, respectively, mice were euthanized, feces were collected for C. muridarum and C. rodentium qPCR (C. rodentium-infected mice only), a complete necropsy was

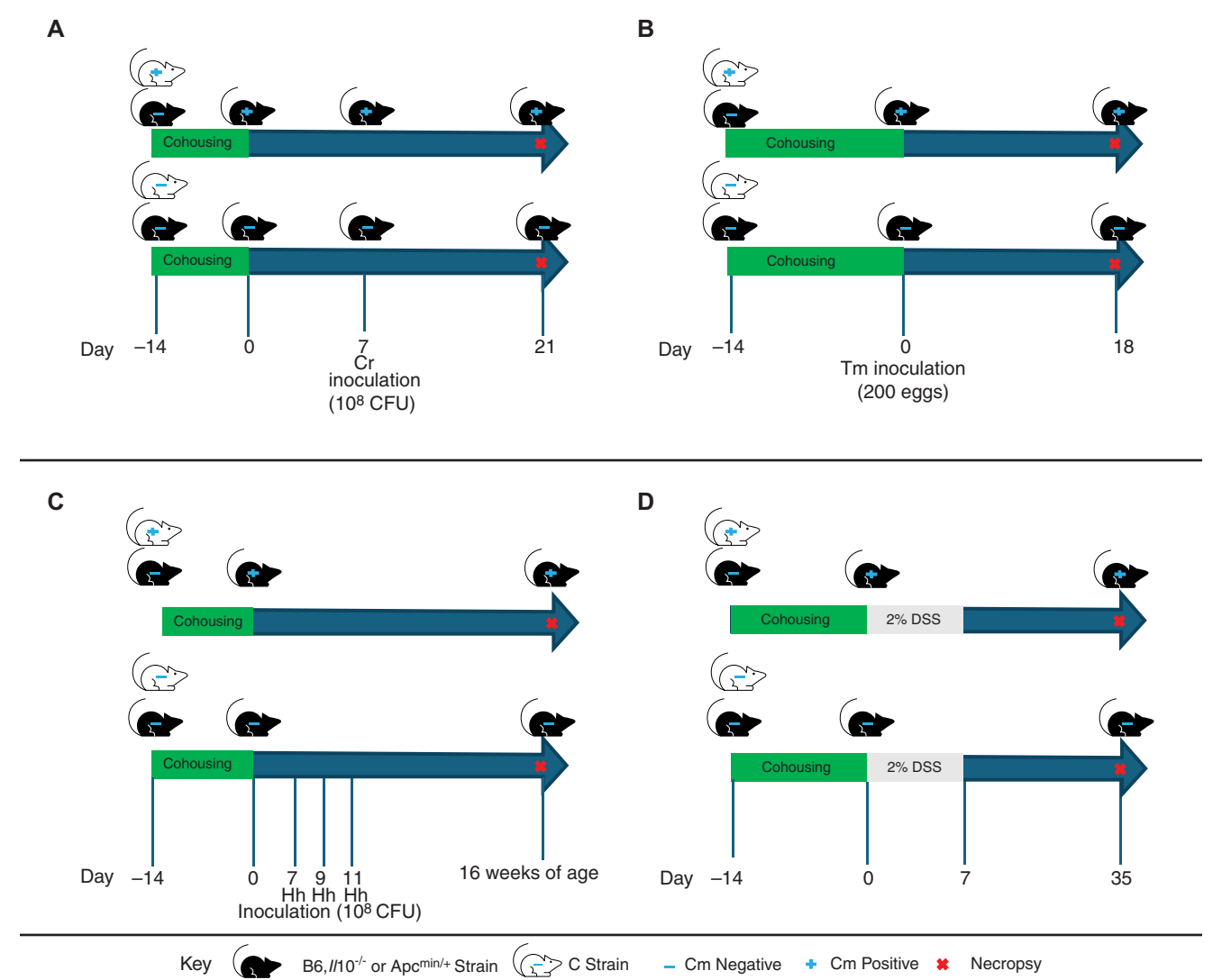


**Figure 1.** Graphical Representation of the Study Design and Timeline. Experimental design and timeline for (A) *Citrobacter rodentium* (Cr), (B) *Trichuris muris* (Tm), (C) *II*10-/-, and (D) Apc<sup>Min/+</sup> experiments. *Citrobacter rodentium*, *T. muris*, and *Helicobacter hepaticus* (Hh) were administered via gavage. DSS was provided in the drinking water.

performed, and the intestinal lesions were scored using a modified published system.  $^{8,9}$ 

 $ll10^{-/-}$  mice (n=32), 16 of which had been cohoused with *C. muridarum*-shedding and the remaining with *C. muridarum*-free C mice, were inoculated with *Helicobacter hepaticus* ( $10^8$  CFU; n=16) or saline (n=16) via orogastric gavage every 2 days for a total of 3 doses at 7 weeks of age. At 16 weeks of age, mice were euthanized, feces were collected for *C. muridarum* and *H. hepaticus* qPCR, a complete necropsy was performed, and the intestinal lesions were scored using a modified scoring system.  $^{10}$ 

Apc<sup>Min/+</sup>mice (n = 8/8; C. muridarum infected/C. muridarum-free) were provided 2% DSS in drinking water for 7 days immediately after cohousing with C. muridarum-infected or C. muridarum-free C mice for 2 weeks. Four weeks post-DSS treatment, mice were euthanized, and the number and location of gross tumors in the gastrointestinal tract (GIT) were counted under a dissecting microscope. Select tumors from each animal were analyzed histologically to confirm malignancy.

**Animals.** Female C57BL/6J (B6; n = 32; 6-week-old; The Jackson Laboratory, Bar Harbor, ME) mice were used for C. rodentium and T. muris experiments (n = 16/experiment); female B6.129P2-II10 $^{tm1Cgn}$ /J ( $II10^{-/-}$ ; n = 32; 4-week-old; The Jackson Laboratory) were used to assess inflammatory bowel disease; and female C57BL/6J-ApcMin/J (Apc $^{Min/+}$ ; n = 16; 4 week old; The Jackson Laboratory) were used to assess tumorigenesis. Female C. muridarum-infected and C. muridarum-free BALB/ cJ (C; n = 4 and n = 3, respectively; greater than 16 week old; The Jackson Laboratory) mice were used for cohousing. Group sizes were selected following review of published studies using each model and based on recommendations of veterinary pathologists and researchers who use these models. In addition, using the resource equation method, a sample size of 8 with 2 groups yields an ANOVA degree of freedom of 14, which is sufficient to demonstrate statistical significance. Experiments were conducted once.

On study initiation all mice were free of ectromelia virus, Theiler meningoencephalitis virus, Hantaan virus, K virus, LDH elevating virus, lymphocytic choriomeningitis virus, mouse adenovirus, murine cytomegalovirus, murine chapparvovirus, mouse hepatitis virus, minute virus of mice, murine norovirus, mouse parvovirus, mouse thymic virus, pneumonia virus of mice, polyoma virus, reovirus type 3, epizootic diarrhea of infant mice (mouse rotavirus), Sendai virus, murine astrovirus-2, Bordetella spp., C. rodentium, C. muridarum, Clostridium piliforme, Corynebacterium bovis, Corynebacterium kutscheri, Filobacterium rodentium (CAR bacillus), Mycoplasma pulmonis and other Mycoplasma spp., Salmonella spp., Streptobacillus moniliformis, Helicobacter spp., Klebsiella pneumoniae and K oxytoca, Pasteurella multocida, Rodentibacter pneumotropicus/heylii, Pseudomonas aeruginosa, Staphylococcus aureus, Streptococcus pneumoniae and Beta-hemolytic Streptococcus spp., Yersinia enterocolitica and Y pseudotuberculosis, Proteus mirabilis, Pneumocystis murina, Encephalitozoon cuniculi, ectoparasites (fleas, lice, and mites), endoparasites (tapeworms, pinworms, and other helminths), protozoa (including Giardia spp. and Spironucleus spp.), Toxoplasma gondii, trichomonads, and dematophytes.

Husbandry and housing. Mice were maintained in autoclaved, individually ventilated, polysulfone shoebox cages with stainless-steel wire-bar lids and filter tops (IVC; number 19; Thoren Caging Systems, Hazleton, PA) on autoclaved aspen chip bedding (PWI Industries, St. Hyacinthe, Quebec, Canada) at a density of no greater than 5 mice per cage. Each cage was provided with a Glatfelter paper bag containing 6 g of crinkled paper strips (EnviroPak; WF Fisher and Son, Somerville, NJ) and a

2-in. square of pulped virgin cotton fiber (Cotton square; Ancare, Bellmore, NY) for enrichment. Mice were fed a natural ingredient, closed-source, γ-irradiated, autoclaved diet (LabDiet 5KA1; PMI, Richmond, IN) ad libitum. 11 All animals were provided autoclaved reverse osmosis acidified (pH 2.5 to 2.8 with hydrochloric acid) water in polyphenylsulfone bottles with stainless-steel caps and sipper tubes (Tecniplast USA, West Chester, PA). Cages were changed every 7 days within a class II, type A2 biologic safety cabinet (LabGard S602-500; NuAire, Plymouth, MN). All cages were housed within a dedicated, restricted-access cubicle, which was maintained on a 12:12-h light:dark cycle (on 6 am:off 6 pm), relative humidity of 30% to 70%, and room temperature of  $72\pm2$ °F (22.2±1.1°C). All cage changing and animal handling were performed by the author (GL). The animal care and use program at Memorial Sloan Kettering Cancer Center (MSK) is accredited by AAALAC International, and all animals are maintained in accordance with the recommendations provided in the Guide for the Care and Use of Laboratory Animals. 12 All animal use described in this investigation was approved by MSK's IACUC in agreement with AALAS' position statements on the Humane Care and Use of Laboratory Animals and Alleviating Pain and Distress in Laboratory Animals. 13,14

Infection of experimental mice with *C. muridarum* via cohousing. The generation of chronically *C. muridarum*-infected C mice was previously described. <sup>1,6</sup> Briefly, *C. muridarum* qPCR-negative C mice were inoculated with  $2.72 \times 10^3$  IFU of a previously isolated *C. muridarum* field strain in 100 µL sucrose-phosphate-glutamic acid buffer (pH 7.2) via orogastric gavage. A new, sterilized gavage needle (22 g × 38.1 mm; Cadence Science, Cranston, RI) was used for each cage.

C. rodentium, T. muris, and H. hepaticus culture and inoculation. C. rodentium (cat. no. 51549; ATCC, Manassas, VA) was cultured in Luria-Bertani broth overnight (cat. no. 3002121; MP Biomedicals, Irvine, CA) at 37 °C with constant shaking. The administered inoculum was confirmed by plating bacteria on MacConkey agar (cat. no. 212123; BD Diagnostics, Franklin Lakes, NJ) and counting the colonies after 14 to 18 hours of incubation. B6 mice were inoculated with  $1 \times 10^9$  CFU in 200  $\mu$ L of PBS via orogastric gavage. A new, sterilized gavage needle (24 g × 38.1 mm; Cadence Science, Cranston RI) was used for each cage.

Embryonated T. muris eggs (Artis Laboratory; Weill Cornell Medicine) were cultivated and maintained in the dark at 4°C, and the inoculum prepared as previously described. <sup>15</sup> Briefly, *T*. muris was maintained in Rag1<sup>-/-</sup> animals. Following euthanize, adult nematodes were isolated from the cecum and proximal colon and cultured at 37 °C in serum-free Roswell Park Memorial Institute Medium 1640 (Corning, Herndon, VA) containing 500 U/mL penicillin and 500 μg/mL streptomycin. Eggs were collected from the culture by filtering through a 70- or 100-µm cell strainer, washed thrice in sterile water, and incubated at room temperature in the dark in a ventilated T75 cell culture flask (Corning, Herndon, VA) for 6 to 8 weeks. Embryonation was confirmed under a dissection microscope, and the eggs were stored at 4 °C in the dark after adjusting the concentration to 200 embryonated eggs per 200 µL in water. B6 mice were inoculated with 200 embryonated T. muris eggs in 200 µL water via oral gavage using a new, sterilized gavage needle (24 g × 38.1 mm; Cadence Science, Cranston, RI).

*H. hepaticus* (51449; ATCC, Manassas, VA) was cultured on blood agar plates (TSA with 5% sheep blood; Thermo Fisher Scientific, Waltham, MA) as previously described. <sup>16</sup> Inoculated plates were placed into a Billups-Rothenberg hypoxia chamber (Embrient, San Diego, CA), and an anaerobic gas mixture

consisting of 80% nitrogen, 10% hydrogen, and 10% carbon dioxide (Airgas, Radnor, PA) was added to create a microaerophilic atmosphere in which the oxygen concentration was 3% to 5%. The concentration of bacterial inoculation dose was determined using a spectrophotometric OD analysis at 600 nm and adjusted to OD at 600 nm readings between 1 and 1.5. Aliquots were then frozen at  $-80\,^{\circ}$ C in *Brucella* broth with 20% glycerol. Frozen aliquots were thawed on ice before oral inoculation.  $II10^{-/-}$  mice were inoculated with  $10^{8}$  CFU of *H. hepaticus* in 0.2 mL of culture broth via orogastric gavage every 2 days for a total of 3 doses. A new, sterilized gavage needle (24 g × 38.1 mm, Cadence Science, Cranston, RI) was used for each cage.

Clinical monitoring. All mice were monitored daily to assess activity, respiratory rate and effort, coat condition and posture, signs of rectal prolapse or diarrhea, and body condition score (BCS). Weights were recorded at the start of each experiment and as needed thereafter based on the BCS. Animals displaying weight loss (20% reduction from baseline) and/or reduced body condition (BCS < 2/5), presenting with dyspnea and/or cyanosis, and/or failing to respond to stimulation were euthanized.

**Fecal collection.** Fecal pellets for PCR were collected ante- or postmortem and pooled by cage for submission. When collected antemortem, the mouse was first lifted by the base of the tail and allowed to grasp onto the wire-bar lid while a 1.5-mL microcentrifuge tube was placed underneath the anus for fecal collection directly into the tube. If the animal did not defecate within 30 s, a fecal sample from the cage floor was collected. Postmortem fecal collection was collected directly from the rectum, if available, or the cage floor.

C. muridarum, C. rodentium, and Helicobacter spp. qPCR assays. DNA and RNA were copurified from fecal samples using the Qiagen DNeasy 96 blood and tissue kit (Qiagen, Santa Clarita, CA). Nucleic acid extraction was performed using the manufacturer's recommended protocol, "Purification of Total DNA from Animal Tissues," with the following buffer volume modifications: 300  $\mu$ L of Buffer ATL + Proteinase K, 600  $\mu$ L of Buffer AL + EtOH, and 600  $\mu$ L of lysate were added to individual wells of the extraction plate. Washes were performed with 600  $\mu$ L of Buffers AW1 and AW2. Final elution volume was 150  $\mu$ L of Buffer AE.

A probe-based PCR assay for *C. muridarum* was designed using IDT's PrimerQuest Tool (Integrated DNA Technologies, Coralville, IA) based on the 16S rRNA sequence of *C. muridarum*, Nigg strain (Accession NR\_074982.1, located in the National Center for Biotechnology Information database). Primer and Probe sequences generated from the PrimerQuest Tool were checked for specificity using NCBI's BLAST (Basic Local Alignment Search Tool). The probe was labeled with FAM and quenched with ZEN and Iowa Black FQ (Integrated DNA Technologies, Coralville, IA). Primer names, followed by associated sequences, were as follows: *C. muridarum\_*For (GTGATGAAGGCTCTAGGGTTG); *C. muridarum\_*Rev (GAGTTAGCCGGTGCTTCTTTA); and *C. muridarum\_*Probe (TACCCGTTGGATTTGAGCGTACCA).

A probe-based PCR assay for *C. rodentium* was designed using IDT's PrimerQuest Tool (Integrated DNA Technologies, Coralville, IA) based on *C. rodentium*'s espB gene sequence of *C. rodentium* (Accession AF\_177537.1, located in the National Center for Biotechnology Information database). Primer and probe sequences generated from the PrimerQuest Tool were checked for specificity using NCBI's BLAST (Basic Local Alignment Search Tool). The probe was labeled with FAM and quenched with ZEN and Iowa Black FQ (Integrated DNA Technologies, Coralville, IA). Primer names, followed by associated sequences, are as

follows: *C. rodentium\_*For (CAGGTATCGCTGATGATGTTACT); *C. rodentium\_*Rev (CAGATTTGCCTTCCGTGTTAAAT); and *C. rodentium\_*Probe (TGCTCAGAAAGCTTCTCAGGTAGCTG).

A proprietary probe-based PCR assay for *Helicobacter* spp. was designed by aligning 16S sequences from the following *Helicobacter* spp.: *H. bilis, H. ganmani, H. hepaticus, H. mastromyrinus, H. muridarum, H. rappini, H. rodentium, H. trogontum,* and *H. typhlonius*. Sequences were aligned using Sequencher 5.4.6 software (Gene Codes). Primers were designed to conserved regions between all species and checked for specificity using NCBI's BLAST (Basic Local Alignment Search Tool). The probe was labeled with HEX and quenched with ZEN and Iowa Black FQ (Integrated DNA Technologies, Coralville, IA).

Real-time qPCR assays were carried out using a real-time PCR system (BioRad CFX machine; Bio-Rad, Hercules, CA). Reactions were run using Qiagen's QuantiNova Probe PCR Kit (Qiagen, Santa Clarita, CA) using the kit's recommended concentrations and cycling conditions. The final concentration was  $1\times$  QuantiNova Master mix,  $0.4~\mu M$  Primers, and  $0.2~\mu M$  FAM or HEX-labeled probe with cycling of 95~C~2~min, followed by 40 cycles of 95~C~5~s, 60~C~30~s.

All reactions were run in duplicate by loading 5  $\mu$ L of template DNA into 15  $\mu$ L of the reaction mixture. A positive and negative, no-template control were included in each run. The positive control was a purified PCR amplicon diluted to produce consistent values of Ct 28. A 16S universal bacterial PCR assay using primers 27\_Forward and 1492\_Reverse was run on all samples to check for DNA extraction and inhibitors. Samples were considered positive if both replicates had similar values and produced a cycle threshold value of less than 40. A sample was called negative if no amplification from the qPCR assay was detected, and a positive amplification from the 16S assay was detected.

Anatomic pathology, lesion scoring, and T. muris infection **confirmation.** Following euthanasia by carbon dioxide overdose, a complete necropsy was performed, and gross lesions were recorded. For all mice except for the ApcMin/+ mice, the GIT from the cecum to rectum was removed and placed in cassettes in a Swiss roll configuration and fixed in 10% neutral buffered formalin for at least 72 hours. Tissues were then processed in ethanol and xylene and embedded in paraffin in a tissue processor (Leica ASP6025; Leica Biosystems, Buffalo Grove, IL). Paraffin blocks were sectioned at 5 µm, stained with hematoxylin and eosin, and evaluated blindly by a board-certified veterinary pathologist (SC). The cecum and colon of C. rodentium- and T. muris-inoculated mice, and Il10-/- mice were graded as described in Tables 1 and 2 using a modified scoring system for each model.<sup>8–10</sup> A composite pathology score was calculated for each mouse by combining all subcategory scores. T. muris infection was confirmed by detecting nematodes histologically.

Tumorigenesis was assessed in the Apc<sup>Min/+</sup> mice following euthanasia after which the GIT from the duodenum to the rectum was removed and placed in a culture dish containing 10% buffered formalin. The entire GIT was then flushed with formalin and opened longitudinally with scissors to expose the lumen for tumor enumeration under a dissecting microscope (Olympus SZX16; Olympus Corp. of the Americas, Center Valley, PA). Select tumors (n = 16) were subsequently submitted for histologic assessment as described above to assess for malignancy.

*Immunohistochemistry.* The entire cecum and colon from each *C. muridarum*-infected colitis model were processed and stained for *Chlamydia* major outer membrane permeabilization (MOMP) using a technique optimized and validated by MSK's

Table 1. Histopathologic Scoring Scheme for Citrobacter rodentium and Trichuris muris (T. muris) Infection in the Colon and Cecum Adapted from Bouadoux et al<sup>8</sup> and Kopper et al<sup>9</sup>

Criterion	0 (absence)	1 (minimal)	2 (mild)	3 (moderate)	4 (severe)
Hyperplasia	None	1.5× normal crypt height	2× normal crypt height	3× normal crypt height	>4× normal crypt height
Goblet cell depletion (Citrobacter rodentium) or hyperplasia (T. muris)	None	5%	5% to 25%	25% to 60%	>60%
Inflammation	None to multifocal rare individual leukocytes scattered in the lamina propria	Multifocal, small discrete clusters of leukocytes in the lamina propria with or without transepithelial leukocyte infiltration	Multifocal, coalescing lamina propria inflammation with or without early submucosal extension	Multifocal, coalescing lamina propria inflammation with multifocal submucosal extension	Multifocal, diffuse transmural inflammation affecting mucosa, submucosa, and deeper layers (muscularis or serosa)
Epithelial defects	None	Occasional dilated glands with luminal cell debris (crypt abscesses)	Multifocal crypt abscesses and surface epithelial tattering and/ or attenuation (intact)	Multifocal erosions or focal ulceration	Multifocal ulcerations
Fibrosis*	None	None or focal, rare in lamina propria	Occasional foci in small segments of the LI, fibroplasia (immature fibroblast proliferation) associated with submucosal inflammation	Multifocal, fibroplasia associated with submucosal inflammation	Multifocal, mature fibrosis with submucosal inflammation and replacement of normal tissue architecture

<sup>\*</sup>Minimal, mild, and moderate fibrosis for the *Citrobacter rodentium* model was defined as 1, 1 to 2, and >2 foci, respectively. Minimal, mild, and moderate fibrosis for the *T. muris* model was defined as 1 to 2, 2 to 5, and >5 foci, respectively.

Table 2. Histopathologic Grading Scheme for the Colon and Cecum from Il10-/- Mice (Adapted from Rogers and Houghton<sup>10</sup>)

Criterion	0 (absence)	1 (minimal)	2 (mild)	3 (moderate)	4 (severe)
Inflammation	None to multifocal rare individual leukocytes scattered in the lamina propria	Multifocal, small discrete clusters of leukocytes in the lamina propria	Multifocal, coalescing lamina propria inflammation with or without early submucosal extension	Multifocal, coalescing lamina propria inflammation with multifocal submucosal extension	Multifocal, diffuse transmural inflammation affecting mucosa, submucosa, and deeper layers (muscularis or serosa)
Hyperplasia	None	1.5× normal crypt height	2× normal crypt height	3× normal crypt height	>4× normal crypt height
Goblet cell depletion	None	5%	5% to 25%	25% to 60%	>60%
Epithelial defects	None	Occasional dilated glands with luminal cell debris (crypt abscesses), and surface epithelial tattering and/or attenuation (intact)	Multifocal crypt abscesses, herniation, and surface epithelial tattering and/or attenuation (intact)	Same changes as 2 plus multifocal erosions or focal ulceration	Same as 3 plus multifocal ulcerations
Crypt Atrophy	None	5% to 25%	25% to 50%	50% to 75%	>75%
Edema	None	Mild segmental expansion of submucosa	Moderate diffuse submucosal +/- mucosal lamina propria expansion	Severe edema of mucosa and submucosa	Transmural; very severe
Dysplasia	None	Mild dysplasia characterized by epithelial cell pleomorphism, plump and attenuated forms, aberrant crypt foci, gland malformation with mild splitting, branching, and infolding, rare cystic dilation	Moderate dysplasia characterized by pleomorphism, early cellular and nuclear atypia, mild piling and infolding, occasional cystic dilation, bulging toward muscularis mucosae and projection into lumen, loss of normal glandular, mucous, or goblet cells, = atypical hyperplasia	Gastrointestinal intraepithelial neoplasia (GIN), severe dysplasia confined to mucosa, features as earlier but greater severity, frequent, and sometimes bizarre mitoses, add 0.5: intramucosal carcinoma (extension of severely dysplastic regions into muscularis mucosae)	Invasive carcinoma: submucosal invasion, or any demonstrated invasion into blood or lymphatic vessels, regional nodes, or other metastasis

Laboratory of Comparative Pathology as a secondary confirmatory method.<sup>1</sup> Briefly, formalin-fixed, paraffin-embedded sections were stained using an automated staining platform (Leica Bond RX; Leica Biosystems, Buffalo Grove, IL). Following deparaffinization and heat-induced epitope retrieval in a citrate buffer at pH 6.0, the primary antibody against Chlamydia MOMP (NB100-65054; Novus Biologicals, Centennial, CO) was applied at a dilution of 1:2,000. A rabbit anti-goat secondary antibody (cat. no. BA-5000; Vector Laboratories, Newark, CA) and a polymer detection system (DS9800; Novocastra Bond Polymer Refine Detection; Leica Biosystems, Buffalo Grove, IL) were then applied to the tissues. The DAB was used as the chromogen, and the sections were counterstained with hematoxylin and examined by light microscopy. Small intestine from an NSG mouse infected with C. muridarum strain Nigg was used as a positive control.<sup>5</sup> Positive MOMP antigen was identified as chromogenic brown immunolabeling under bright field microscopy

In situ hybridization (ISH) was conducted on the large intestine of a subset of *C. muridarum*-positive  $Il10^{-/-}$  animals (n = 8)in which the MOMP immunohistochemistry (IHC) signal was absent. Briefly, the target probe was designed to detect region 581 to 617 of C. muridarum str. Nigg complete sequence, NCBI Reference Sequence NC\_002620.2 (1039538-C1; Advanced Cell Diagnostics, Newark, CA). The target probe was validated on reproductive tracts from mice experimentally inoculated with C. muridarum strain Nigg. 5 Slides were stained on an automated stainer (Leica Bond RX; Leica Biosystems, Buffalo Grove, IL) with RNAscope 2.5 LS Assay Reagent Kit-Red (322150; Advanced Cell Diagnostics, Newark, CA) and Bond Polymer Refine Red Detection (DS9390; Leica Biosystems, Buffalo Grove, IL). Control probes detecting a validated positive housekeeping gene (mouse peptidylprolyl isomerase B, Ppib to confirm adequate RNA preservation and detection; 313918; Advanced Cell Diagnostics, Newark, CA) and a negative control, Bacillus subtilis dihydrodipicolinate reductase gene (dapB to confirm absence of nonspecific staining; 312038; Advanced Cell Diagnostics, Newark, CA) were used. Positive RNA hybridization was identified as discrete, punctate chromogenic red dots under bright field microscopy.

**Statistical analysis.** All data sets were determined to be normally distributed using the Kolmogorov-Smirnov test. Mann-Whitney U (Wilcoxon rank sum) tests were used to compare colitis scores between C. muridarum-infected and C. muridarum-free control mice infected with C. rodentium and T. muris. The Kruskal-Wallis test for multiple comparisons was used to compare pathology scores between C. muridarum-infected, H. hepaticus-infected, coinfected, and control  $II10^{-/-}$  mice. An unpaired t test was used to compare gross tumor numbers between C. muridarum-infected and C. muridarum-free Apc $^{Min/+}$ mice. For all tests, statistical significance was set as a  $P \le 0.05$ . Analysis and graphical representations were performed and created in Prism 9 (version 9.3.0; GraphPad Software, San Diego, CA) for Windows.

#### Results

C. rodentium colitis model. Mice were confirmed to be infected with C. rodentium only or C. rodentium and C. muridarum as expected at the experimental endpoint via qPCR and IHC. A single C. muridarum- and C. rodentium-infected mouse was found dead 10 days postinoculation. Histopathology revealed a moderate to marked, multifocal necroulcerative and suppurative colitis. This mouse was excluded from analysis as the lesions may represent an atypical presentation of C. rodentium infection

or may have been caused by an unidentified etiology. All remaining animals remained clinically normal for the duration of the study. The colons of mice infected with both *C. rodentium* and *C. muridarum* had statistically significantly lower composite and individual scores for inflammation and goblet cell depletion when compared with colons from *C. rodentium*-inoculated, *C. muridarum*-free mice (Figure 2). Colitis was characterized in the *C. muridarum*-free mice as diffuse and moderate to marked, while *C. muridarum*-positive mice had mild to moderate colitis. Both groups had infiltration of the lamina propria by lymphocytes, plasma cells, and histiocytes with submucosal extension (Figure 2B and C).

**T. muris colitis model.** All mice in each group were confirmed to be infected with only *T. muris* or both *T. muris* and *C. muridarum* at the end of the experiment by histology and qPCR. No mice developed signs of illness for the duration of the experiment. Mice coinfected with *T. muris* and *C. muridarum* showed no significant score differences in the cecum and colon for any individual component or the composite score when compared with mice infected only with *T. muris* (Table 3). Colitis in both groups was characterized as multifocal and moderate with infiltration of the lamina propria by lymphocytes, plasma cells, eosinophils, and histiocytes with submucosal extension. *T. muris* larvae were readily appreciated in the lumen of all mice examined (Figure 3).

1/10-/-colitis model (H. hepaticus-infected and -free). Mice were confirmed C. muridarum-free or C. muridarum-infected at euthanasia by qPCR as expected except 2 animals representing a single mouse in the C. muridarum-only group and another in the C. muridarum + H. hepaticus coinfected group despite having been qPCR positive after cohousing. Given the initial positive qPCR results after cohousing and similar intestinal pathology to other mice in the group, these mice were included in the analysis. None of the mice developed signs of illness for the duration of the experiment. MOMP staining of the cecum and colon was negative for Il10<sup>-/-</sup> mice cohoused with a C. muridarum-shedding mouse for 2 weeks despite the fact that most of these mice were qPCR positive. ISH was also performed on cecum and colon sections to confirm the presence of *C. muridarum*. Staining was detected in the colon of all C. muridarum-infected animals, except for 1 of the 2 aforementioned qPCR-negative mice representing the C. muridarum+ H. hepaticus coinfected group (Figure 4).

The individual pathology component scores as well as the composite scores for both the cecum and colon are provided in Figure 5; representative images demonstrating select pathologic changes are provided in Figure 4. While infecting *Il*10-/mice with *C. muridarum* did not impact the composite pathology score in the cecum compared to controls, it did result in significant colonic pathology equivalent in magnitude to that resulting from *H. hepaticus* infection in this model. *H. hepaticus* caused significant pathology in both the cecum and colon. Infection of *Il*10-/mice with both bacterial species did not increase the composite colonic pathology score more than the changes resulting from infection with either species alone.

The composite score difference between *C. muridarum*-free and -infected mice in the colon was a result of a significant increase in inflammation, epithelial defects, crypt atrophy, and goblet cell depletion following *C. muridarum* infection. While epithelial hyperplasia was observed in the *Il*10<sup>-/-</sup> mice following *C. muridarum* infection, the change was not significant. Crypt atrophy was also a principal component of the pathologic changes resulting from *C. muridarum* infection, regardless as to whether the *Il*10<sup>-/-</sup>were infected with *H. hepaticus*. Crypt

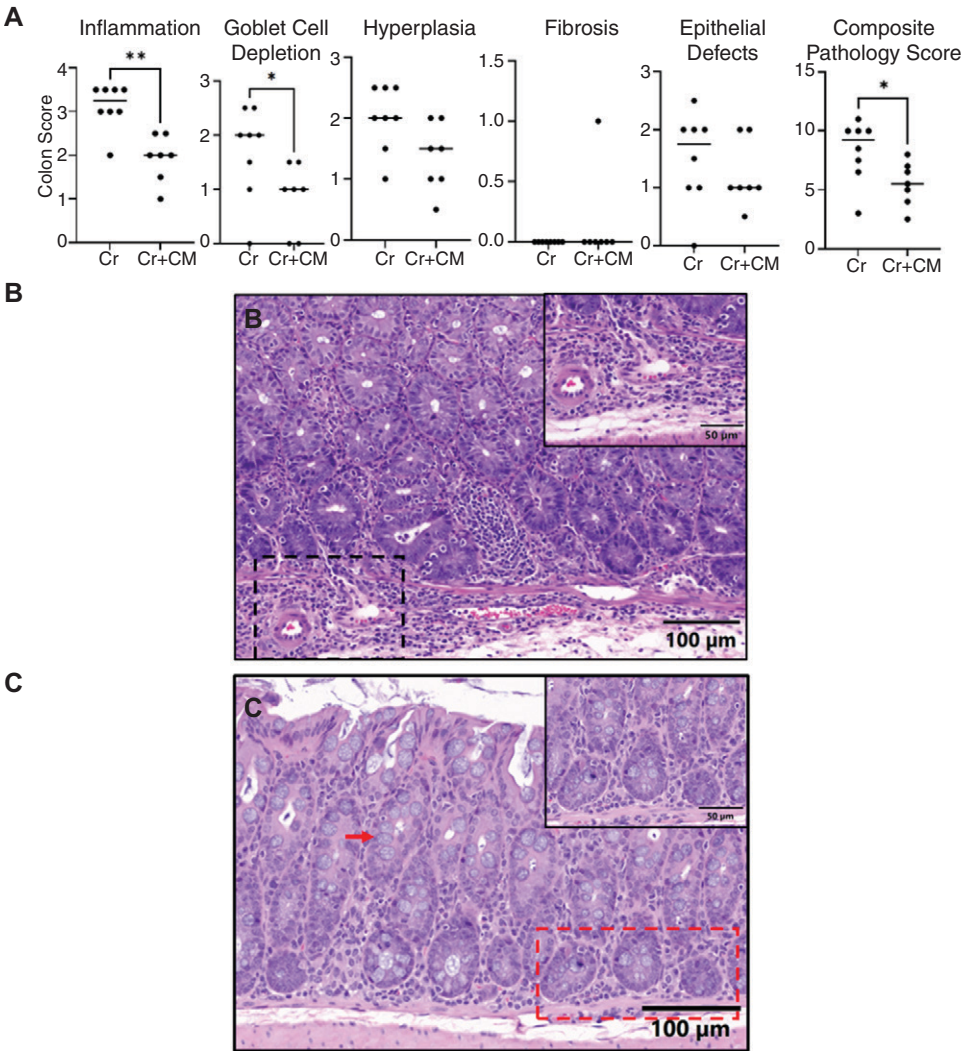


Figure 2. The Effects of Chlamydia muridarum (Cm) on Citrobacter rodentium (Cr)-Induced Colitis. (A) Individual and composite colitis scores of female C57BL/6J mice infected with only Citrobacter rodentium or infected with both Citrobacter rodentium and C. muridarum (n = 8 mice/group) 14 d post-Citrobacter rodentium infection. Composite pathology scores were calculated by combining scores from all subcategories. The crossbar represents the median lesion score for each parameter. (B and C) Representative H&E-stained images of colons from mice infected with only Citrobacter rodentium (B) or with both Citrobacter rodentium and C. muridarum (C) 14 d post-Citrobacter rodentium infection. (B) Moderate to marked mucosal and submucosal inflammation with infiltration of the lamina propria (inset), moderate crypt hyperplasia, and mild goblet cell depletion in affected crypts in the colon of a Citrobacter rodentium-infected, C. muridarum-free mice with a composite pathology score of 10 (10× magnification; inset:  $40 \times$  magnification). (C) Less severe mucosal inflammation (inset), reduced crypt hyperplasia, and less goblet cell depletion (red arrow) in the colon of a Citrobacter rodentium-infected, C. muridarum-positive mouse with a composite pathology score of 7 ( $10 \times$  magnification; inset,  $10 \times 10 \times 10^{-10}$  magnification; inset,  $10 \times 10^{-10}$  magnification). (C) Less severe mucosal inflammation (inset), reduced crypt hyperplasia, and less goblet cell depletion (red arrow) in the colon of a Citrobacter rodentium-infected, C. muridarum-positive mouse with a composite pathology score of 7 ( $10 \times 10 \times 10^{-10}$  magnification). (T) magnification; inset,  $10 \times 10^{-10}$  magnific

Table 3. Pathology Scores Assigned to the Cecum and Colon of Mice Infected with *Trichuris muris* with and without *Chlamydia muridarum* 

	Cecum		Colon	
Category	T. muris	C. muridarum + T. muris	T. muris	C. muridarum + T. muris
Inflammation	$2.56 \pm 0.50$	$2.31 \pm 0.46$	$2.25 \pm 0.46$	$2.56 \pm 0.32$
Epithelial hyperplasia	$1.81 \pm 0.26$	$1.75 \pm 0.46$	$1.5 \pm 0.38$	$1.75 \pm 0.38$
Goblet cell hyperplasia	$1.25 \pm 0.27$	$1.0 \pm 0.53$	$1.38 \pm 0.35$	$1.19 \pm 0.26$
Epithelial defects	$1.81 \pm 0.46$	$1.5 \pm 0.80$	$1.31 \pm 0.46$	$1.69 \pm 0.37$
Fibrosis	$0.25 \pm 0.46$	$0.44 \pm 0.62$	$0.25 \pm 0.46$	$0.13 \pm 0.35$
Composite pathology score	$7.69 \pm 1.56$	$7.0 \pm 2.55$	$6.69 \pm 1.89$	$7.31 \pm 0.88$

Pathology scores (mean  $\pm$  SD) of all criteria of the cecum and colon of female C57BL/6J mice infected with *T. muris* or coinfected with *T. muris* and *C. muridarum* (n=8 mice/group) 18 d post-*T. muris* infection following cohousing with a *C. muridarum*-shedding or *C. muridarum*-free mouse for 2 wk. None of the score differences in any category or the composite scores in either the cecum or colon were significantly different.

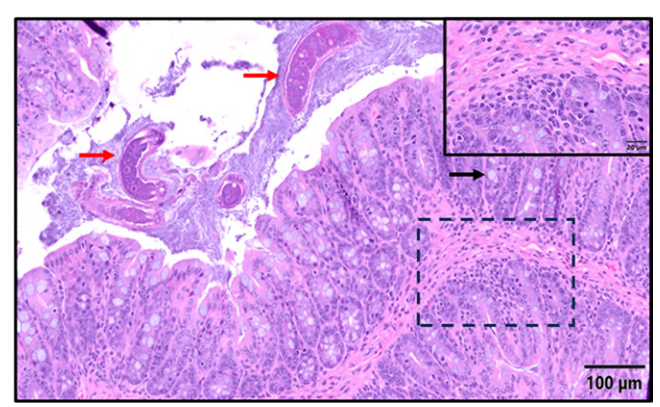


Figure 3. Histopathology of the Colon from a *Chlamydia muridarum*-Free Mouse Infected with *Trichuris muris* 18 d Post-*T. muris* Infection. Representative hematoxylin and eosin-stained image of the colon from a mouse infected with *T. muris* 18 d following cohousing with a *C. muridarum*-free mouse for 2 wk (composite pathology score = 7.5). A multifocal infiltrate of lymphocytes, eosinophils, and plasma cells is present in the lamina propria with submucosal extension (inflammation score = 3; inset) in association with mild to moderate hyperplasia and mild goblet cell hypertrophy (goblet cell hypertrophy score = 1; black arrow) in affected crypts and intraluminal *T. muris* larvae (red arrows). ( $10 \times magnification$ ; inset:  $60 \times magnification$ ).

atrophy was inconsistently observed in *Il*10<sup>-/-</sup>mice infected with only *H. hepaticus*. While *H. hepaticus* infection of *Il*10<sup>-/-</sup> mice resulted in edema, edema was not a component of the pathology associated with *C. muridarum* infection in this model.

While *C. muridarum* infection of the *Il*10<sup>-/-</sup>mouse led to a minimal increase in the cecal composite pathology score, these increases were principally a result of inflammation and epithelial defects; however, none of these differences were statistically significant. Cecal edema, epithelial hyperplasia, and goblet cell hyperplasia were the major pathologic features that were more severe in the *H. hepaticus*-infected as compared with the *C. muridarum*-infected *Il*10<sup>-/-</sup> mice.

ApcMin/+ DSS model of intestinal neoplasia. Mice were confirmed C. muridarum-free or C. muridarum-infected at euthanasia by qPCR as expected. C. muridarum MOMP immunolabeling was also detected in tumors and normal intestinal mucosa (data not shown). None of the mice developed signs of illness for the duration of the experiment. As expected, DSS exposure resulted in increased tumorigenesis in the colon. Tumors were identified grossly as raised mucosal nodules (Figure 6B). C. muridarum-infected ApcMin/+mice had statistically fewer identifiable colonic tumors as compared with C. muridarum-free ApcMin/+mice (Figure 6A). The number of small intestinal and cecal tumors were not significantly different between C. muridarum-free and C. muridarum-infected ApcMin/+mice. Overall tumor burden per mouse was reduced in the presence of C. muridarum. All C. muridarum-free ApcMin/+mice exposed to 2% DSS developed gross intestinal tumors; however, one of the C. muridarum-infected mice failed to develop a colonic tumor. Two and 4 C. muridarum-free mice failed to develop small intestinal and cecal tumors, respectively, as compared with the C. muridarum-infected mice where one mouse failed to develop any small intestinal tumors, and none of the 8 mice developed cecal neoplasia. All tumors evaluated histologically were classified as adenomas (Figure 6C).

#### **Discussion**

Biosecurity is an integral and essential component of contemporary research mouse colony management as it is well recognized that there is a plethora of infectious agents that, while they may not cause clinical disease and/or pathology, can nevertheless confound research in which infected mice are used. It is for these reasons that most institutions maintain their rodent colonies, especially mice, in barrier facilities implementing specific husbandry and operational processes focused on keeping out a host of excluded infectious agents that may adversely impact the research for which the animals are used. Ascertaining which agents should be excluded is becoming ever more challenging as novel agents are identified, and the impact of the microbiota and agents that had historically been considered commensals is continuing to evolve.

Our group recently discovered and reported on the reemergence and surprisingly high prevalence of the bacterium C. muridarum in research mouse colonies and showed that C. muridarum causes silent, but persistent infection of the large intestine of various commonly used murine strains and stocks. 1,6 We further confirmed alterations of innate and adaptive immune responses following exposure by its natural route of infection.<sup>6</sup> These findings lead to the question as to whether *C. muridarum* can have a significant impact on the research in which infected mice are used, particularly those analyzing the intestine. A recent study<sup>7</sup> revealed that *C. muridarum* altered responses in the commonly used murine DSS-induced colitis model of inflammatory bowel disease. C. muridarum-infected DSS-treated mice had less pathology through an IL-22-dependent pathway. Therefore, we speculated that C. muridarum would have a significant impact on other mouse models used to study gastrointestinal disease. We elected to assess C. muridarum's impact on 4 commonly used murine models, 3 of which are used to interrogate intestinal inflammation and infection with the bacterium C. rodentium and the parasite *T. muris*, as well as the genetically engineered IL-10 knockout mouse model in which gut inflammation develops spontaneously in association with specific intestinal consortia. The DSS-treated ApcMin/+ mouse model of intestinal neoplasia was also assessed. While the study's aim was not to determine the mechanism(s) by which C. muridarum, if shown to influence any or all of these models, altered the models, but rather to aid us and others in determining the significance of its presence and assess whether the impact is sufficient to consider exclusion from some or all murine mouse colonies. These models were selected on their frequency of use as well as the likelihood, based on C. muridarum's pathophysiology, to alter the model phenotype.

The C. rodentium mouse model of bacterial infection is commonly used to enhance the understanding of bacterial pathogenesis and mucosal immunity, especially as it relates to enterohemorrhagic and enteropathogenic Escherichia coli infection.<sup>8</sup> Infection of B6 mice with 10<sup>8</sup> to 10<sup>9</sup> CFU of C. rodentium results in transient colonic crypt hyperplasia typically lasting 2 to 3 weeks.<sup>8</sup> Initially, *C. rodentium* colonizes the colon and rapidly expands after infection. By day 7 postinfection, the bacterial load plateaus, and by day 10, the infection starts to clear with complete clearance observed by 2 to 3 weeks.8 Hallmark histologic changes associated with the developing colitis is the colonic crypt hyperplasia. 8 We demonstrated that coinfecting C. muridarum-infected mice with C. rodentium significantly decreased the severity of colitis when compared with C. muridarum-free mice inoculated with the same C. rodentium dose. C. muridarum and C. rodentium-coinfected mice had significantly less inflammation and goblet cell depletion, and while the magnitude of the epithelial hyperplasia and cell defects was not statistically different, both these parameters were also reduced in coinfected mice. We speculate that local and systemic upregulation of IFNy, IL-17, and IL-22 following C. muridarum infection

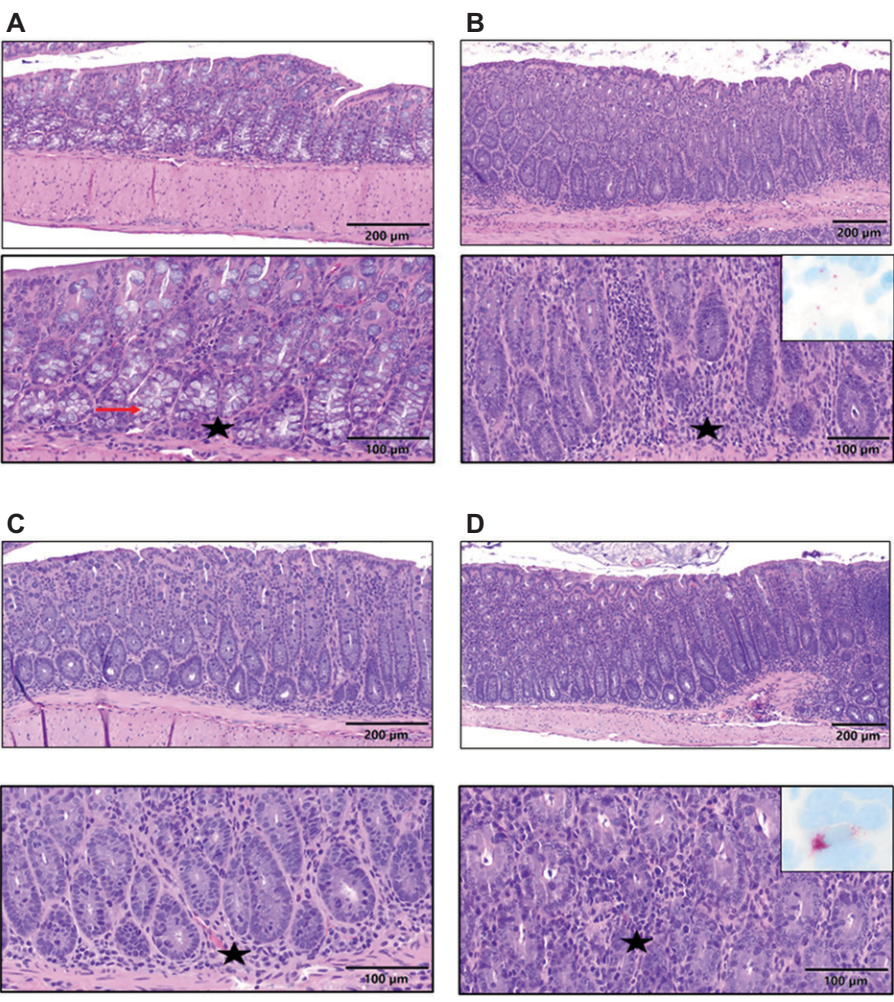


**Figure 4.** Colonic Lesions in *Helicobacter hepaticus*-Infected and -Free *Il*10<sup>-/-</sup> Mice Coinfected with *Chlamydia muridarum*. Representative images from are from (A) Colon of a *C. muridarum*- and *H. hepaticus*-free *Il*10<sup>-/-</sup> mouse showing occasional lymphocytes in the lamina propria (black star) and abundant goblet cells (red arrow; composite score=2). (B) Colon from a *C muridarum*-infected *Il*10<sup>-/-</sup> mouse with moderate colitis (black star), mild mucosal hyperplasia and moderate goblet cell atrophy (composite score=11). Inset: *C. muridarum* ISH signal (red) in mucosal epithelium. (C) Colon from an *H. hepaticus*-infected, *C. muridarum*-free *Il*10<sup>-/-</sup> mouse showing moderate to marked colitis (black star) with mild to moderate mucosal hyperplasia and moderate goblet cell atrophy (composite score=11.5). (D) Colon from a *C. muridarum* and *H. hepaticus* coinfected *Il*10<sup>-/-</sup> mouse with epithelial hyperplasia and colitis (black star) and moderate goblet cell atrophy (composite score=10). Inset: *C. muridarum* ISH signal (red) in mucosal epithelium. H&E stain (10× and 20× magnification; insets: 40× magnification).

resulted in the reduction of *C. rodentium*-induced colitis.<sup>6</sup> Th1, Th17 and Th22 and their respective cytokines, IFNγ, IL-17A, and IL-22, respectively, mediate host response to *C. rodentium* infection.<sup>17</sup> IFNγ-deficient mice fail to clear *C. rodentium* as a consequence of reduced activation of *C. rodentium*-antigenspecific T cells and the subsequent reduction in antibacterial IgG production and macrophage phagocytosis.<sup>18</sup> IL-17 and IL-22, in particular, are essential for protection against *C. rodentium*.<sup>8</sup> The latter is protective by upregulating epithelial repair and production of antimicrobial peptides.<sup>17</sup> We excluded a single *C. muridarum* and *C. rodentium* coinfected mouse from the study, which was unexpectedly found dead 10 days after *C. rodentium* inoculation with unusual and unexpected lesions.

We also examined the impact of *C. muridarum* on the *T. muris*-induced colitis model in B6 mice. This model of human whipworm infection is useful for dissecting host-nematode interactions. <sup>19</sup> A low dose of 50 ova elicits a Th1 response in which B6 mice become persistently infected and develop a chronic colitis, while mice gavaged with a high dose of 200 ova develop a Th2 response resulting in worm expulsion within 21 days. <sup>19,20</sup> We elected to evaluate *C. muridarum*'s impact on the

latter model as we hypothesized the Th1 response and increase in IFNy elicited by a preexisting C. muridarum infection would increase susceptibility to *T. muris*. However, there were no differences detected. All pathology criteria scored as well as the composite score were similar in C. muridarum-free as compared with C. muridarum-infected mice. The Th1 cytokines IL-12, IL-18, and IFNy induce susceptibility to T. muris infection. 19 IFNy is thought to be the principal mediator as depletion results in expulsion of T. muris in susceptible strains. 21 IL-18 and IL-12 induce IFNγ production.<sup>22</sup> Il12b<sup>1-/-</sup> and Il18<sup>-/-</sup> animals are resistant to infection.<sup>23</sup> Resistance in Il12<sup>-/-</sup> mice is primarily mediated by reducing IFNγ production; however, resistance in Il18-/- is a result of IL-13 suppression inhibiting the Th2 response.<sup>23</sup> Administration of recombinant IL-12 or IL-18 to a resistant strain results in susceptibility to infection, further implicating the Th1-cell response is key to susceptibility to chronic *T. muris* infection.<sup>23</sup> The observed lack of differences in our study may reflect C. muridarum's other effects. Although C. muridarum infection elicits an increase in IFNy, it also increases IL-22 and IL-17.6 IL-22 deficiency leads to susceptibility to T. muris infection in normally resistant mice.<sup>24</sup> Loss of IL-22 decreases goblet

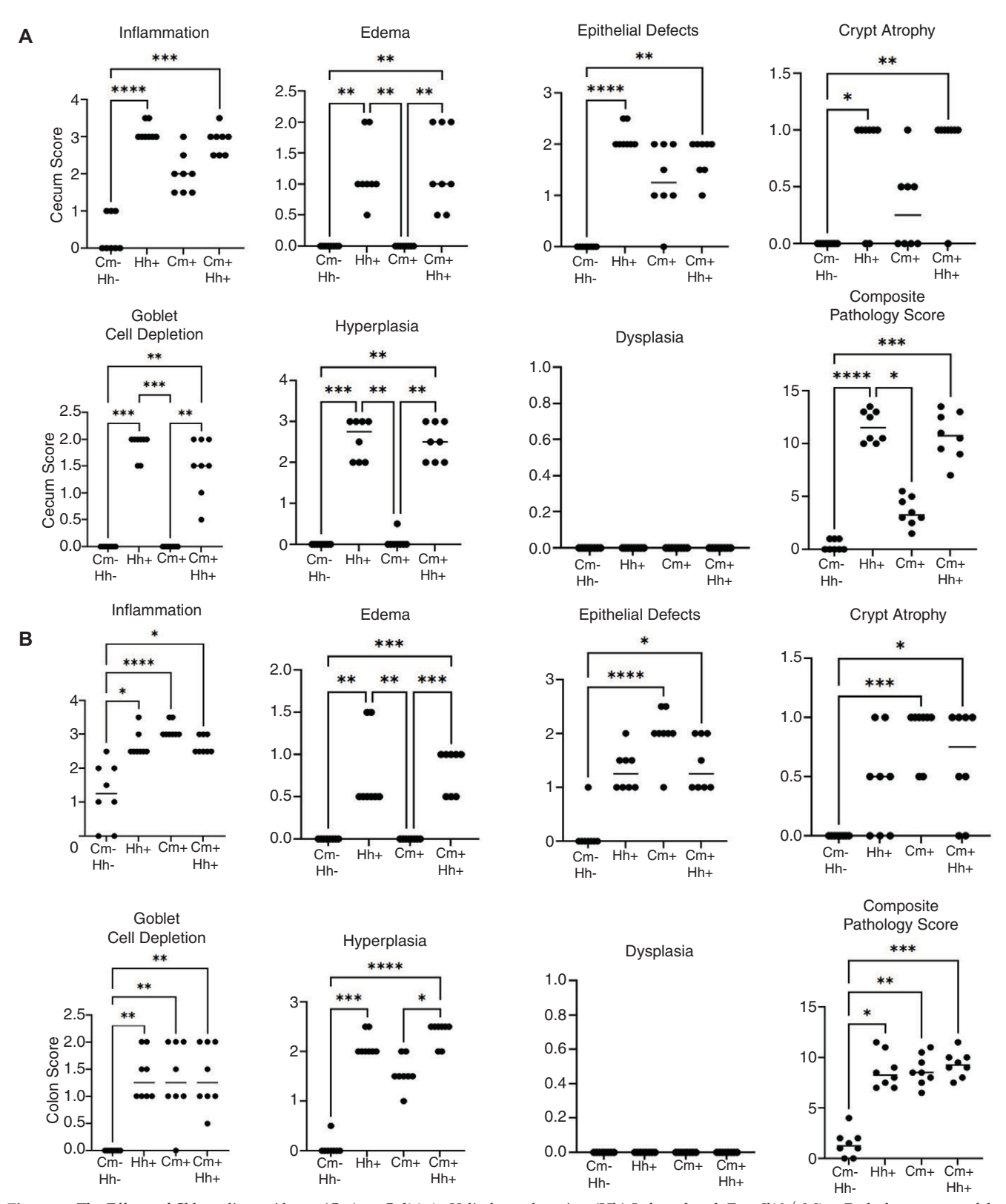


**Figure 5.** The Effects of *Chlamydia muridarum* (Cm) on Colitis in *Helicobacter hepaticus* (Hh)-Infected and -Free  $Il10^{-/-}$  Mice. Pathology scores of the (A) cecum and (B) colon of female  $Il10^{-/-}$  mice (control), infected with *H. hepaticus*, infected with *C. muridarum*, or coinfected with *C. muridarum* and *H. hepaticus* (n=8 mice/group). Scores for inflammation, edema, epithelial defects, crypt atrophy, goblet cell depletion, hyperplasia, dysplasia, and composite scores of all score parameters. The crossbars on the graphs indicate the median lesion scores for each parameter. \*,  $P \le 0.05$ ; \*\*,  $P \le 0.01$ ; \*\*\*,  $P \le 0.001$ ; \*\*\*,  $P \le 0.$ 

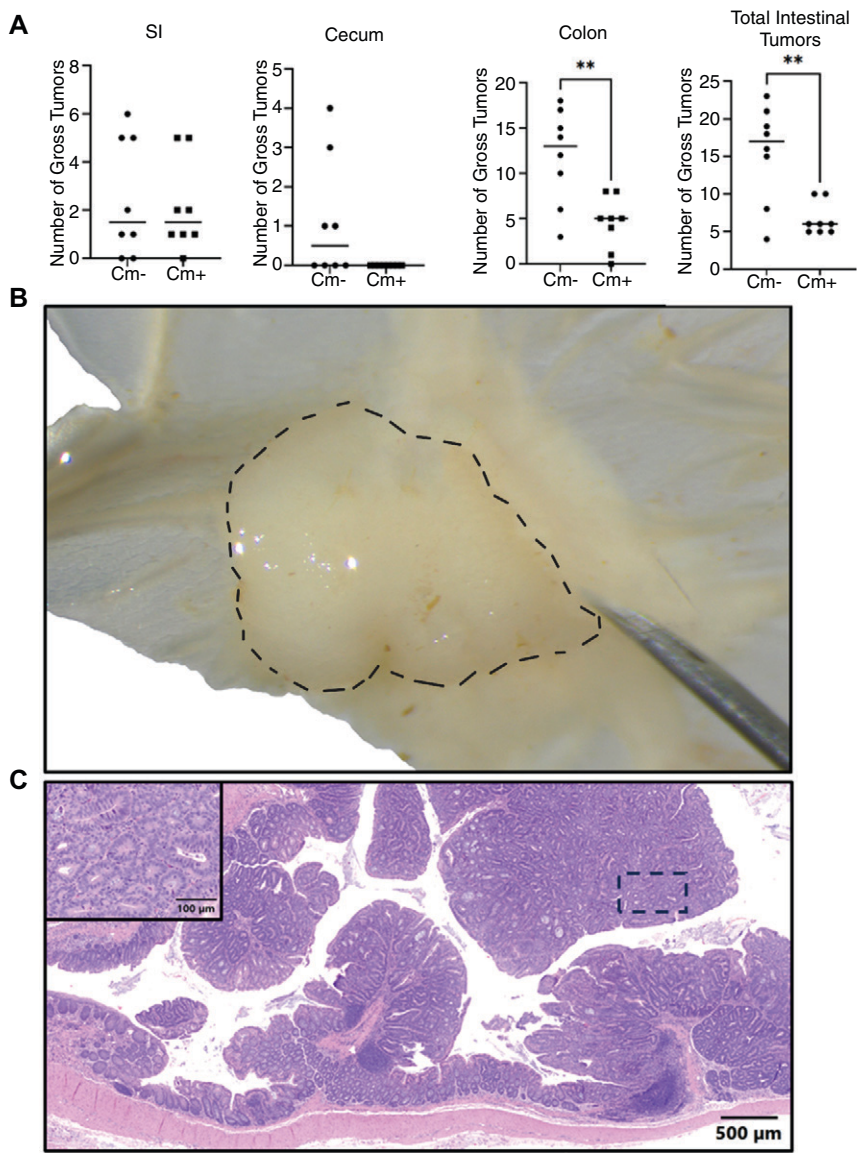


**Figure 6.** Colonic Tumors in the Small Intestine, Cecum and Colon of *C. muridarum*-Infected (Cm+) and -Free (Cm-) DSS Treated, Apc<sup>Min/+</sup> mice. (A) Gross tumor count in the small intestine, colon, cecum, and total tumor count per mouse at necropsy of female control *C. muridarum*-free Apc<sup>Min/+</sup> mice or *C. muridarum*-infected Apc<sup>Min/+</sup> mice at 4-wk post 2% DSS treatment (n = 8/group). The crossbar represents the median lesion score for each parameter. \*\*, P < 0.005. (B) Representative photo of a gross tumor (outlined by a dashed line) in the colon of Apc<sup>Min/+</sup> mice 4-wk post 2% DSS treatment at necropsy. (C) Representative H&E-stained images of a colonic tumor from Apc<sup>Min/+</sup> mice 4-wk post-2% DSS treatment. Tumors were characterized as adenomas (2× magnification; inset: 20× magnification).

cell proliferation and mucous production impairing worm expulsion.  $^{24}$  Therefore, even though *C. muridarum* infection leads to an increase in production of IFN $\gamma$ , the increase in IL-22 may have counteracted its impact. Given these results, it would be interesting to evaluate *C. muridarum*'s impact on the low-dose B6 model as the heightened Th1-cell response could increase pathology and worm burden.

*C. muridarum*'s impact on the *Il*10<sup>-/-</sup> model of gut inflammation was also examined as it has a clinicopathologic phenotype influenced by the microbiota.<sup>25–27</sup> The loss of IL-10 leads to colitis as a result of an aberrant immune response in the presence of specific agents such as *H. hepaticus*.<sup>25</sup> We demonstrated that *C. muridarum* induced colitis of similar magnitude to that caused by *H. hepaticus*. Therefore, *C. muridarum* can be added to the list of agents capable of inducing colitis in the model. Interestingly, coinfection with both agents did not lead to colitis of greater severity than either bacterium caused alone. This finding may reflect that both bacteria induce colitis by the same mechanism.

IFNγ, IL-17, and IL-22 are upregulated in the absence of IL-10.<sup>25,28</sup> IFNγ has historically been linked to the development of colitis in *H. hepaticus*-infected *Il*10<sup>-/-</sup> mice as intestinal inflammation is reduced following administration of neutralizing monoclonal antibodies.<sup>29</sup> Recent studies<sup>30</sup> have shown that mice deficient in both IFNy and IL10 still developed colitis following H. hepaticus infection suggesting that colitis is likely induced by other pathways. Although IL-17 was linked to colitis in this model, there are more recent reports of mice deficient in both IL-17 and IL-10 developing more severe colitis than mice deficient only in IL-10.27 IL-22 is also overexpressed in Il10<sup>-/-</sup> mice and is associated with the colitis phenotype.<sup>28</sup> Helicobacter spp.-infected mice deficient in both IL-22 and IL-10 remained colitis free suggesting that IL-22 is a major driver of colitis in this model.<sup>28</sup> Given that IFNγ, IL-17and IL-22 are upregulated following C. muridarum infection, it is not surprising that *C. muridarum* is sufficient to induce colitis in *Il*10<sup>-/-</sup> mice in the absence of *H. hepaticus*.<sup>6</sup>

Interestingly, 2 of 16 Il10<sup>-/-</sup> mice were negative for *C. muridarum* by qPCR at euthanasia despite being qPCR positive following cohousing 70 days prior. One of these 2 mice was coinfected with H. hepaticus while the other was H. hepaticus free. Both were singly housed after cohousing, which could have contributed to a reduction in *C. muridarum* burden to undetectable levels by qPCR as they would not have been continuously exposed to C. muridarum by a C. muridarum-shedding cage mate. Despite negative qPCR results, intestinal pathology was similar to other C. muridarum-positive animals. Interestingly, all C. muridarum-infected Il10-/-were also MOMP IHC negative, which was not observed in any of the other models we evaluated, although *C. muridarum* was detectable in most of the *Il*10<sup>-/-</sup> mice evaluated via ISH. Of the 2 mice negative for C. muridarum by qPCR, one was also negative by ISH. Collectively, these findings indicate that the *C. muridarum* burden in the large intestine decreases temporally in this model with only trace amounts of C. muridarum nucleic acid detectable in the colonic mucosa by the end of the experimental period. Given that IL-10 is a potent anti-inflammatory cytokine that modulates immune responses, it is plausible that the exaggerated inflammatory response led to the clearance of most chlamydial inclusions from the intestines. This notion is supported by prior studies<sup>31</sup> using *Il*10<sup>-/-</sup> mouse models, which demonstrated a progressive reduction in C. trachomatis burden in the lungs beginning 7 days postinfection. Although proinflammatory cytokine levels were not assessed in the colonic mucosa of C. muridarum-infected Il10<sup>-/-</sup> mice, it is well established that upregulation of IFNy production by epithelial cells plays a critical role in host defense by depleting intracellular tryptophan, an essential nutrient for Chlamydia replication within host tissues.<sup>32</sup> Future studies should elucidate the immunoregulatory pathways influenced by C. muridarum in the colon of *Il*10<sup>-/-</sup>mice.

Finally, we assessed the impact of *C. muridarum* infection on the DSS-treated ApcMin/+ mouse of colonic neoplasia. Importantly, C. muridarum infection significantly decreased tumor burden in the model. We elected to use the DSS-treated model as DSS exposure stimulates colonic neoplasia rather than the small intestinal neoplasia that predominates in untreated ApcMin/+mice.33,34 As C. muridarum infection preferentially colonizes the large intestine, we speculated that it would be more likely to influence the DSS-treated model.<sup>6</sup> Although the specific mechanism by which DSS impacts colonic tumorigenesis is unknown, the induction of colonic neoplasia is likely influenced by the resulting colitis.<sup>33</sup> Our findings are not surprising considering C. muridarum alleviated DSS-induced colitis by stimulating IL-22 production, and the cytokine has been shown to be protective in chemically-induced models of tumorigenesis by decreasing inflammation.<sup>7,21,35</sup> Interestingly, IL-22 can also be tumorigenic as Il22-/-ApcMin/+mice develop fewer tumors as compared with Il22+/+ApcMin/+mice.35,36 The mechanism is believed to be a result of the epithelial turnover induced by IL-22 suggesting that multiple pathways could impact tumorigenesis in C. muridarum-infected, DSS-treated ApcMin/+ mice. 36 It remains unknown whether C. muridarum infection could influence neoplasia in untreated Apc<sup>Min/+</sup> mice. C. rodentium infection of ApcMin/+mice resulted in increased colonic neoplasia; the mechanism was thought to result from increased epithelial turnover.<sup>37</sup> Although C. muridarum infection has not been reported to induce epithelial hyperplasia, we observed epithelial hypertrophy in C. muridarum-infected Il10<sup>-/-</sup> mice.<sup>4</sup> Future research could examine the impact of C. muridarum in the untreated Apc<sup>Min/+</sup> mouse model.

C. muridarum infection significantly impacted 3 of the 4 gastrointestinal models evaluated in this study providing further and compelling evidence that C. muridarum status should be considered when using these models. One reason to consider excluding C. muridarum is the sensitivity of available diagnostics for its detection and, more importantly, the relative ease by which C. muridarum can be successfully eradicated from most mouse strains using antibiotic therapy.<sup>38</sup> This contrasts with other prevalent murine infectious agents, such as MNV, that, while ideally should be excluded, the process of establishing MNV-free colonies would be extremely challenging in that numerous unique strains of mice present in many colonies would need to be rederived. Careful consideration should also be given to using previously C. muridarum-infected, antibiotic-treated mice as research subjects as the impact of prior *C. muridarum* infection is unknown. Ideally, offspring of treated mice should be used, although epigenetic multigenerational effects remain possible.

# Acknowledgments

We thank Jacqueline "Jackie" Candelier, Sockie Jiao, and the staff of the Laboratory of Comparative Pathology for their assistance with necropsies, histology, immunohistochemistry and in situ hybridization assays, Mohd Anees Ahmed for his assistance with *C. rodentium* culture and infection and Mengze Lyu for his assistance with *Helicobacter hepaticus* culture.

### **Conflict of Interest**

Anthony Mourino and Mert Aydin are employees of Jackson Laboratories, a company that produces and distributes research models and provides research services. David Artis has contributed to scientific advirsory boards at Pfizer, Nemagene and the Kenneth Rainin Foundation. The other authors have no competing interest to declare.

Funding

This work was funded in part by the ACLAM Foundation. The Laboratory of Comparative Pathology is supported in part by NIH Grant P30 CA008748. Hiroshi Yano and David Artis are supported by The Allen Discovery Center program, a Paul G. Allen Frontiers Group advised program of the Paul G. Allen Family Foundation, the AGA Research Foundation, the WCM-RAPP Initiative, Cure for IBD, the Weill Cornell Medicine Jill Roberts Institute for Research in IBD, the Kenneth Rainin Foundation, the Sanders Family Foundation, the Rosanne H. Silbermann Foundation, the Glenn Greenberg and Linda Vester Foundation, the Crohn's & Colitis Foundation (937437), and the National Institutes of Health (K99AI180354, DK126871, AI151599, AI095466, AI095608, AI142213, AR070116, AI172027, DK132244).

### **References**

- Mishkin N, Ricart Arbona RJ, Carrasco SE, et al. Reemergence of the murine bacterial pathogen *Chlamydia muridarum* in research mouse colonies. *Comp Med.* 2022;72(4):230–242.
- Elwell C, Mirrashidi K, Engel J. Chlamydia cell biology and pathogenesis. Nat Rev Microbiol. 2016;14(6):385–400.
- 3. Albers TM, Henderson KS, Mulder GB, Shek WR. Pathogen prevalence estimates and diagnostic methodology trends in laboratory mice and rats from 2003 to 2020. *J Am Assoc Lab Anim Sci.* 2023;62(3):229–242.
- Yeruva L, Spencer N, Bowlin AK, Wang Y, Rank RG. Chlamydial infection of the gastrointestinal tract: a reservoir for persistent infection. *Pathog Dis.* 2013;68(3):88–95.
- St Jean SC, Ricart Arbona RJ, Mishkin N, et al. *Chlamydia mu-ridarum* infection causes bronchointerstitial pneumonia in NOD.Cg-PrkdcscidIl2rgtm1Wjl/SzJ (NSG) mice. *Vet Pathol*. 2024;61(1):145–156.
- Mishkin N, Carrasco SE, Palillo M, et al. Chlamydia muridarum causes persistent subclinical infection and elicits innate and adaptive immune responses in C57BL/6J, BALB/cJ and J: ARC(S)

- mice following exposure to shedding mice. Comp Med. 2024; 74(6):373–391
- 7. Wang X, Zeng HC, Huang YR, He QZ. *Chlamydia muridarum* alleviates colitis via the IL-22/occludin signal pathway. *Biomed Res Int*. Preprint posted online December 20, 2020.
- Bouladoux N, Harrison OJ, Belkaid Y. The mouse model of infection with Citrobacter rodentium. Curr Protoc Immunol. 2017; 119:19.15.1–19.15.25.
- 9. Kopper JJ, Theis KR, Barbu NI, et al. Comparison of effects of *Trichuris muris* and spontaneous colitis on the proximal colon microbiota in C3H/HeJ and C3Bir IL10<sup>-/-</sup> mice. *Comp Med*. 2021;71(1):46–65.
- Rogers AB, Houghton J. Helicobacter-based mouse models of digestive system carcinogenesis. Methods Mol Biol. 2009;511: 267–295.
- 11. Thurlow RW, Arriola R, Soll CE, Lipman NS. Evaluation of a flash disinfection process for surface decontamination of gamma-irradiated feed packaging. *J Am Assoc Lab Anim Sci.* 2007;46(4):46–49.
- Institute for Laboratory Animal Research. Guide for the Care and Use of Laboratory Animals. 8th ed. The National Academies Press; 2011.
- AALAS Position Statement on the Humane Care and Use of Laboratory Animals. Comp Med. 2017;67(6):548–548.
- 14. Turner P, Kirchain S, DiVincenti L, et al. ACLAM Position Statement on Pain and Distress in Research Animals. *J Am Assoc Lab Anim Sci.* 2016;55(6):821.
- 15. Artis D, Villarino A, Silverman M, et al. The IL-27 receptor (WSX-1) is an inhibitor of innate and adaptive elements of type 2 immunity. *J Immunol.* 2004;173(9):5626–5634.
- Xu M, Pokrovskii M, Ding Y, et al. c-MAF-dependent regulatory T cells mediate immunological tolerance to a gut pathobiont. Nature. 2018;554(7692):373–377.
- Silberger DJ, Zindl CL, Weaver CT. Citrobacter rodentium: a model enteropathogen for understanding the interplay of innate and adaptive components of type 3 immunity. *Mucosal Immunol*. 2017;10(5):1108–1117.
- Shiomi H, Masuda A, Nishiumi S, et al. Gamma interferon produced by antigen-specific CD4+ T cells regulates the mucosal immune responses to Citrobacter rodentium infection. Infect Immun. 2010;78(6):2653–2666.
- Klementowicz JE, Travis MA, Grencis RK. Trichuris muris: a model of gastrointestinal parasite infection. Semin Immunopathol. 2012;34(6):815–828.
- 20. Antignano F, Mullaly SC, Burrows K, Zaph C. *Trichuris muris* infection: a model of type 2 immunity and inflammation in the gut. *JoVE*. 2011;(51):e2774.
- Else KJ, Finkelman FD, Maliszewski CR, Grencis RK. Cytokine-mediated regulation of chronic intestinal helminth infection. J Exp Med. 1994;179(1):347–351.
- Cliffe LJ, Grencis RK. The *Trichuris muris* system: a paradigm of resistance and susceptibility to intestinal nematode infection. *Adv Parasitol*. 2004;57:255–307.
- 23. Helmby H, Takeda K, Akira S, Grencis RK. Interleukin (IL)-18 promotes the development of chronic gastrointestinal helminth

- infection by downregulating IL-13. *J Exp Med.* 2001;194(3): 355–364.
- 24. Turner JE, Stockinger B, Helmby H. IL-22 mediates goblet cell hyperplasia and worm expulsion in intestinal helminth infection. *PLoS Pathog.* 2013;9(10):e1003698.
- Keubler LM, Buettner M, Hager C, Bleich A. A multihit model: colitis lessons from the interleukin-10-deficient mouse. *Inflamm Bowel Dis.* 2015;21(8):1967–1975.
- Whary MT, Taylor NS, Feng Y, et al. Lactobacillus reuteri promotes Helicobacter hepaticus-associated typhlocolitis in gnotobiotic B6.129P2-IL-10(tm1Cgn) (IL-10(-/-)) mice. Immunology. 2011;133(2):165–178.
- Hsu CC, Paik J, Treuting PM, et al. Infection with murine norovirus 4 does not alter *Helicobacter*-induced inflammatory bowel disease in IL10<sup>-/-</sup> mice. *Comp Med.* 2014;64(4):256–263.
- Gunasekera DC, Ma J, Vacharathit V, et al. The development of colitis in II10(-/-) mice is dependent on IL-22. *Mucosal Immunol*. 2020;13(3):493–506.
- Kullberg MC, Ward JM, Gorelick PL, et al. Helicobacter hepaticus triggers colitis in specific-pathogen-free interleukin-10 (IL-10)-deficient mice through an IL-12- and gamma interferondependent mechanism. Infect Immun. 1998;66(11):5157–5166.
- Kullberg MC, Rothfuchs AG, Jankovic D, et al. Helicobacter hepaticus-induced colitis in interleukin-10-deficient mice: cytokine requirements for the induction and maintenance of intestinal inflammation. Infect Immun. 2001;69(7):4232–4241.
- Yang X, Gartner J, Zhu L, Wang S, Brunham RC. IL-10 gene knockout mice show enhanced Th1-like protective immunity and absent granuloma formation following *Chlamydia trachomatis* lung infection. *J Immunol*. 1999;162(2):1010–1017.
- 32. Wang L, Hou Y, Yuan H, Chen H. The role of tryptophan in *Chlamydia trachomatis* persistence. *Front Cell Infect Microbiol*. 2022;12:931653.
- 33. Tanaka T, Kohno H, Suzuki R, et al. Dextran sodium sulfate strongly promotes colorectal carcinogenesis in Apc(Min/+) mice: inflammatory stimuli by dextran sodium sulfate results in development of multiple colonic neoplasms. *Int J Cancer.* 2006;118(1): 25–34.
- Cooper HS, Everley L, Chang WC, et al. The role of mutant Apc in the development of dysplasia and cancer in the mouse model of dextran sulfate sodium-induced colitis. *Gastroenterology*. 2001;121(6):1407–1416.
- 35. Hernandez P, Gronke K, Diefenbach A. A catch-22: interleukin-22 and cancer. *Eur J Immunol*. 2018;48(1):15–31.
- Huber S, Gagliani N, Zenewicz LA, et al. IL-22BP is regulated by the inflammasome and modulates tumorigenesis in the intestine. *Nature*. 2012;491(7423):259–263.
- 37. Newman JV, Kosaka T, Sheppard BJ, Fox JG, Schauer DB. Bacterial infection promotes colon tumorigenesis in Apc(Min/+) mice. *J Infect Dis.* 2001;184(2):227–230.
- 38. Palillo MB, Carrasco SE, Mishkin N, et al. Assessment of antimicrobial therapy in eradicating chlamydia muridarum in research mice: immune status and its impact on outcomes. *J Am Assoc Lab Anim Sci.* 2025;64(1):76–88.